


# Experimental comparison of absorber and conductive floor automotive near field antenna measurement systems

cambridge.org/mrf

F. Saccardi<sup>1</sup> , F. Mioc<sup>1</sup>, A. Scannavini<sup>1</sup>, P. O. Iversen<sup>2</sup>, J. Estrada<sup>3</sup>, M. Edgerton<sup>4</sup>, J. A. Graham<sup>5</sup> and L. J. Foged<sup>1</sup>

## Industrial and Engineering Paper

**Cite this article:** Saccardi F, Mioc F, Scannavini A, Iversen PO, Estrada J, Edgerton M, Graham JA, Foged LJ (2022). Experimental comparison of absorber and conductive floor automotive near field antenna measurement systems. *International Journal of Microwave and Wireless Technologies* **14**, 689–700. <https://doi.org/10.1017/S1759078721001343>

Received: 7 May 2021

Revised: 23 August 2021

Accepted: 5 September 2021

First published online: 20 October 2021

### Key words:

Automotive; spherical near field; multi-probe; absorbers; perfect electric conductor; ground plane; truncation

### Author for correspondence:

F. Saccardi,

E-mail: [francesco.saccardi@mvg-world.com](mailto:francesco.saccardi@mvg-world.com)

<sup>1</sup>Microwave Vision Italy SRL, Via dei Castelli Romani 59, 00071, Pomezia, Italy; <sup>2</sup>Orbit/FR's Corporate HQ, 650 Louis Drive Suite 100, 18974 Warminster, PA, USA; <sup>3</sup>MVG Inc., 450 Franklin Gateway Suite 100, 30067 Marietta, GA, USA; <sup>4</sup>GM Proving Ground, 3300 General Motors Rd, 48380, Milford, MI, USA and <sup>5</sup>GM Technical Fellow Antenna Development and Performance (Retired), Linden, Michigan (MI), USA

### Abstract

Large truncated spherical near-field systems with conductive or absorbing floors are typically used in the measurement of the performances of vehicle-installed antennas. The main advantage of conductive floor systems is the ease of accommodation of the vehicle under test, but their performances are affected by the interaction with the reflecting ground floor. Instead, absorbing-based systems emulating free-space conditions minimize the effect of the interaction with the floor, but generally require longer setup times, especially at lower frequencies (70–400 MHz), where bulky absorbers are typically used to improve reflectivity levels. Considering scaled measurements of a vehicle model, the performances of these two typical implementations are analyzed in the 84–1500 MHz range and compared to free-space measurements. Absorbers with different dimensions and reflectivity have been installed in the scaled measurement setup, and measured data have been investigated with proper post-processing to verify the applicability to realistic systems. Figures of merit of interest for automotive applications, like gain and partial radiated powers, have been compared to free-space to evaluate the impact of different scenarios.

## Introduction

Spherical near-field systems installed in shielded anechoic chambers are typically used in modern automotive antenna measurements [1–5]. Such systems are truncated at or close to the horizon, to host the vehicle under test while limiting the size/cost of the chamber. As shown in Fig. 1, the vehicle to be tested is placed on a metallic floor or on a floor covered by absorbing materials. The latter solution is intended to emulate a free-space environment [4] and is a key factor to perform accurate measurements at low frequencies (down to 70 MHz). The availability of the free-space response also enables easy emulation of car behaviors over realistic automotive floors with commercially available tools [6–8]. As described in [9], such emulations are more complex when a conductive ground is used, and such types of floors are a good approximation of realistic grounds (such as asphalts) only in a limited number of situations. Moreover, conductive ground measurements suffer from a relevant interaction between the conductive floor and the measurement system; thus, the quality of the measurements could be degraded, especially at lower frequencies. On the other hand, the main advantages of these types of systems are the ease of the accommodation of the vehicle under test, and the simplification of the NF/FF transformation [10], enabling the mitigation of the truncation errors [11].

In this paper, measurements over conductive and absorbing floors using a scaled vehicle model and a scaled automotive system are compared to free-space measurements of the same test object, to assess the performances of different configurations. The analysis is carried out considering (scaled) frequencies relevant to automotive applications in the 84–1500 MHz range. Two types of scaled absorbers of different sizes and reflectivity are used to emulate the behaviors of the realistic full-scale 48-inch and 18-inch height absorbers. Forty-eight-inch absorbers usually have a low reflectivity down to 70–80 MHz [12] but, due to their size, they are difficult to move, and the vehicle normally needs to be raised from the floor to avoid the shadowing effect. Consequently, more time is generally needed to setup a measurement with 48-inch absorbers, unless special car-feeding mechanisms are employed as shown in [4]. On the other hand, the nominal reflectivity of the 18-inch absorbers is relatively high at lower frequencies (70–400 MHz). Nevertheless, their use at such frequencies would offer some advantages including cost reduction and optimization of the time needed to setup the measurements. For these reasons, they have been also included in this analysis. To deal with

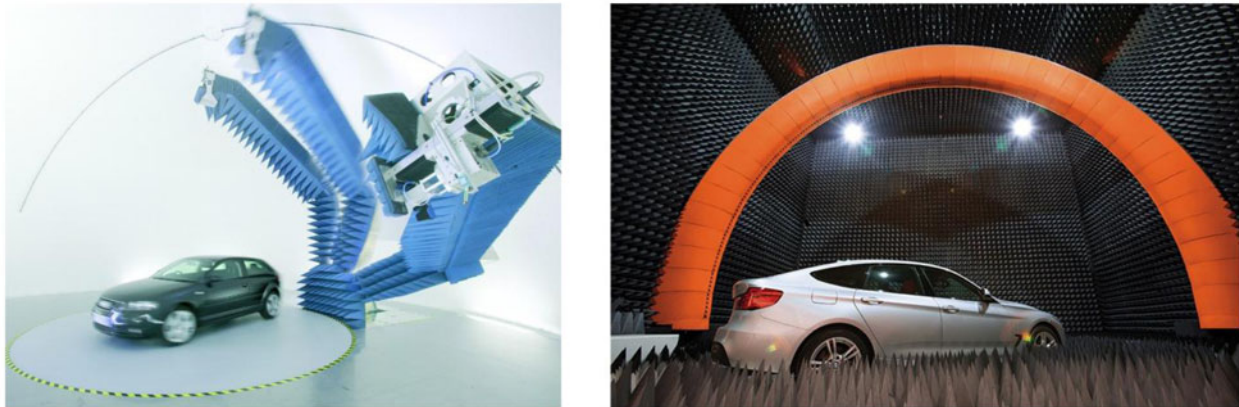


Fig. 1. Examples of automotive spherical NF systems: single probe with conductive floor (left); multi-probe with absorbing floor (right).

the poor reflectivity of the 18-inch absorbers at a lower frequency, the scaled measurements are also performed with the vehicle raised from the floor; spatial filtering [9, 13] is then applied to measured data in post-processing to mitigate the effect of the interaction with the floor.

An earlier version of this paper was presented at the EuCAP 2020 Conference and was published in its Proceedings [1]. In [1], only one antenna position was investigated, and only gain and pattern results were presented. In this contribution, the analysis has been extended to three antenna positions within the body of the scaled vehicle, and additional interesting figure of merits regarding the partial radiated powers have been included.

### Experiment description

Scaled automotive measurement test scenarios with different floors like those shown in Fig. 1 have been implemented to compare experimentally their measurement performances. The scaled-model technique [14] has been applied. Such a technique is based on the basic concept that the EM performance of a generic antenna system depends on its dimensions in terms of wavelengths (electrical size). Therefore, if the physical dimensions are divided by a factor  $N$  and the frequency is multiplied by the same factor  $N$ , the electromagnetic behavior is maintained for fully metallic objects. The application of the scaled-model technique to this scaled automotive measurement allows to consider a full-spherical free-space data as a baseline/reference to assess the influence of different floor scenarios.

A 1:12 scaled-car model (Morris Minor 1000 of 1965) fed by patch antennas has been measured in the StarLab-18 GHz (SL18 GHz) multi-probe system in different configurations (see Fig. 2).

The SL18 GHz is comprised of two interleaved probe arrays capable of performing measurements in the frequency ranges from 0.4 to 6 and 6 to 18 GHz, respectively. The measurement radius of the system is 45 cm.

Three similar wideband patch antennas have been installed in three different positions on the car model (see Fig. 2): close to the windshield, on the rear part of the roof, and on the hood of the scaled vehicle, respectively. Different antenna positions have been chosen to investigate different interactions with the ground floors. For example, the hood antenna is expected to interact more with the floor than the ones installed on the windshield or on the roof. In each measurement, only one patch is fed while the other

two are terminated with a matched load. Measurements have been performed in the frequency band 1.008–18 GHz. With the considered  $N=12$  scaling factor, the performed measurements are equivalent to the ones of a full-size vehicle (real dimensions of  $L \times W \times H = 3.76 \times 1.55 \times 1.52$  m) measured in a system with a 5.4 m radius in the 84–1500 MHz band.

The scaled vehicle has been first measured in free-space over the full sphere, as shown in the top-left part of Fig. 2. Such measurements have been considered as a reference to assess the influence of different floor scenarios.

To emulate the two typical automotive system floor conditions shown in Fig. 1, a metallic ground has been introduced inside the system. Such metallic ground floor is composed of a 75 cm diameter turntable which rotates with the antenna, and of a fixed metallic part which extends outside the system. Conductive contacts have been included in the junction between the two metallic parts to ensure the electrical continuity. The metallic floor is placed 11 cm below the center of the scanner (corresponding to a position of 1.32 m in real dimensions) to emulate real automotive systems where the top of the car is located close to the center of the spherical scan (see schematic illustrations in Fig. 3). This displacement allows for measurements down to approximately  $\theta = 100^\circ$  (i.e.  $10^\circ$  below the horizon). Measurements over a conductive floor have been carried out with this extended setup by placing the scaled vehicle at floor level (see Fig. 2, bottom-right and Fig. 3, left). In the data processing, the metallic floor is assumed to be a Perfect Electric Conductor (PEC).

Absorber-based systems have been emulated considering two types of absorbing materials:

- 4-inch pyramidal absorbers (Fig. 2, top-right);
- 1.5-inch convoluted absorbers (Fig. 2 bottom-left and bottom-center).

The nominal reflectivity at normal incidence of the considered absorbers is reported in Table 1. It should be noted that with this type of approach, only the physical dimensions of the absorbers are properly scaled. The conductivity (losses) of the absorbers cannot be scaled (as it should be, according to the scale-model method [14]). In this specific case, the reflectivity of the considered scaled absorbers is 5–10 dB higher than the one of the full-size (12-time larger) absorbers [12] meaning that a worst-case scenario is considered with respect to the real one. Nevertheless, this has been assumed to be a reasonable approximation, providing a representative emulation of the real scenario.

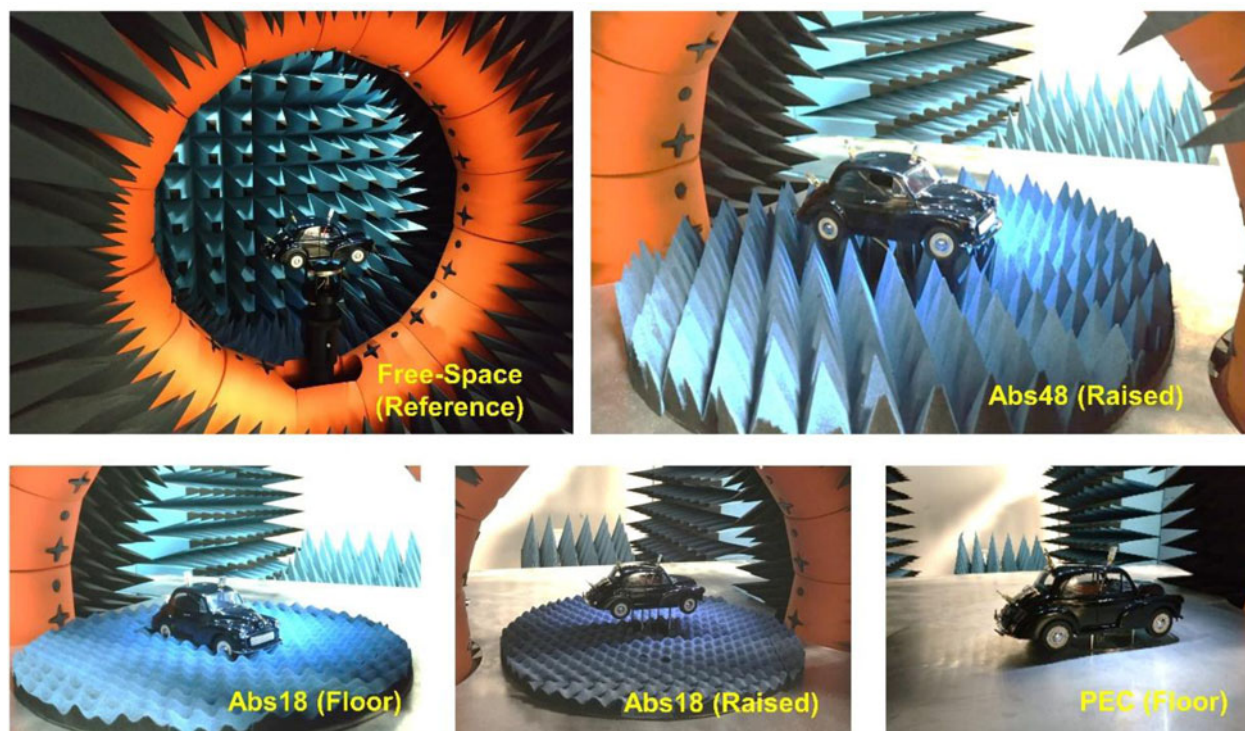


Fig. 2. Scaled vehicle measured in free-space and on the different floor scenarios: 48-inch (Abs48) and 18-inch (Abs18) scaled absorbers and metallic floor (PEC).

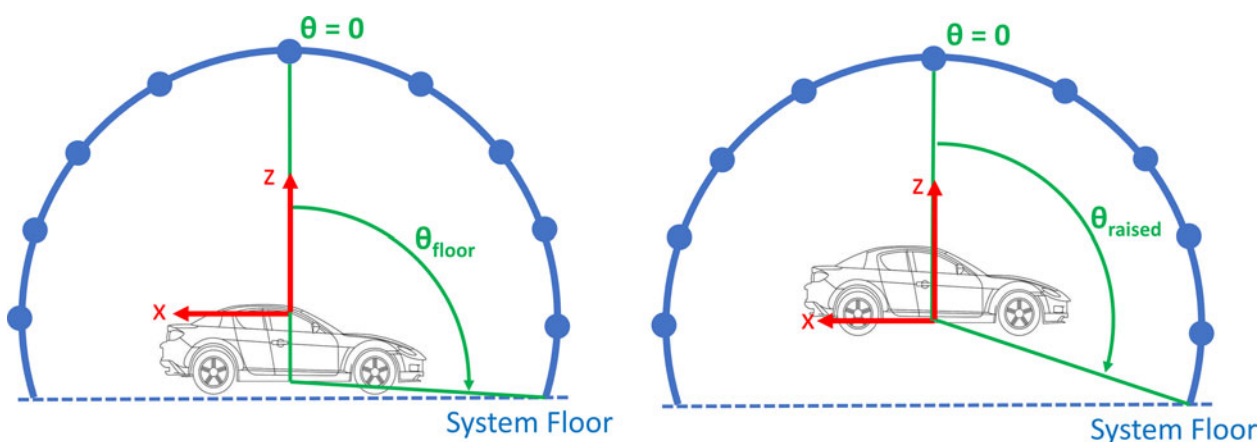


Fig. 3. Schematic illustrations of floor and raised configurations ( $\theta_{\text{raised}} > \theta_{\text{floor}}$ ).

As depicted in Fig. 2, the absorbers have been placed only on the top of the turntable as done in any full-scale system of this kind [4]. The remaining part of the metallic floor has not been covered by absorbers as done in other types of absorber-based systems [4].

With the applied scaling factor ( $N = 12$ ), the 4-inch absorbers are equivalent to 48-inch (Abs48) height full-size absorbers, which are typically used down to 70–80 MHz. Due to the height of these absorbers, the car has been raised from the floor by 7.5 cm (0.9 m in real dimensions) to avoid the shadowing effect of the absorbers (see Fig. 2, top-right and Fig. 3, right). This is a conventional displacement when absorbers with this height are used [4].

The 1.5-inch absorbers are instead equivalent to 18-inch (Abs18) height full-size absorbers. The reduced height of these absorbers enables the placement of the car directly on the floor,

as depicted in Fig. 1 (left), simplifying the setup phase of the measurement. Such absorbers are typically used starting from 400 to 500 MHz. Despite this, they have been used over the whole tested frequency range (84–1500 MHz), since they could be an attractive solution at lower frequencies (80–500 MHz) due to their cost advantage and ease of installation with respect to the 48-inch absorbers. Scaled measurements with the 18-inch absorbers have been performed with the vehicle at two different distances from the ground:

- Vehicle on the floor (floor configuration) as shown in Fig. 2 (bottom-left); performed over the whole frequency range (84–1500 MHz);
- Vehicle raised 7.5 cm (equivalent to 0.9 m) from the floor (raised configuration) as shown in Fig. 2 (bottom-center); performed in the lower frequency range (84–500 MHz).



**Table 1.** Nominal reflectivity at normal incidence of the considered absorbers [12]

Measured frequency [GHz]	Scaled (1:12) frequency [MHz]	4-inch absorbers (Abs48) [dB]	1.5-inch absorbers (Abs18) [dB]
1	83	n/a	n/a
3	250	-30	n/a
6	500	-35	-20
10	833	-40	-30
15	1250	-45	-35
18	1500	-50	-36

In this case, the raised measurements have been performed to verify if the expected deterioration of performance caused by the poor reflectivity of the 18-inch absorbers at lower frequencies can be improved by increasing the electrical separation of the vehicle from the ground and applying a spatial filtering in a post-processing step (see [9, 13] for more details). Such raised measurements have not been performed above 500 MHz because of the well-established behavior of the 18-inch absorbers at such frequencies.

Simplified illustrations of the floor and raised configurations are shown in Fig. 3. The reference coordinate system is reported in red and is in both cases centered in the center of the measurement sphere. It is highlighted that when the car is raised, a larger equivalent  $\theta$  area can be covered ( $\theta_{\text{raised}} > \theta_{\text{floor}}$ ).

As described in detail in [15], each measurement setup has been gain-calibrated independently, using horn reference antennas, and applying the gain substitution technique [2, 14].

## Results

Calibration, radiation patterns, gain and partial radiated powers results of the scaled measurements performed with the different floor scenarios are reported in this section.

It is remarked that for each figure of merit, the influences of the considered floors are evaluated by comparison with the free-space scenario. There are two main reasons for the choice of the free-space scenario as the reference one. First, the object of this study is the evaluation of the influence of different kinds of floors on the measured radiating performance of the vehicle-installed antennas, hence a reflection-free reference scenario is the logical choice. Second, measuring the free-space response is often a requirement because, as shown in [6, 7], it allows for a straightforward emulation of vehicle responses over any type of ground (eventually including PEC as shown in [7]). As shown in [9], the same any-ground emulations from measurement performed in PEC conditions are instead much more complex and, in many cases, they do not allow to properly approximate the wanted ground response. Nevertheless, it should also be pointed out that in some cases, the PEC response is directly considered a good approximation of some driving grounds, such as wet asphalts. For this reason, the comparison between free-space and PEC scenarios that are presented in this paragraph should not be intended as an estimation of the accuracy of the PEC-based systems, but as a metric to emphasize the differences between these two types of measurements scenarios.

### Gain calibration

The accuracy of the gain calibration of measurement setups with different floors has been described in detail in [15]. In this

paragraph, only the main concepts and results are recalled for completeness.

Each measurement setup has been calibrated using the gain substitution technique [2, 14]. Reference antennas with known gain/efficiency have been measured to calibrate the different scenarios. The considered reference antennas are two horns which have been measured in the lower and upper frequency ranges of the measurement system, respectively. The substitution technique has been applied considering the efficiency and gain of reference antennas. Both gain and efficiency are power-related quantities that can be used to measure the losses of the measurement systems and hence calibrated them. In particular, the substitution method based on the efficiency provides more accurate calibrations than the one based on gain because the efficiency, unlike the gain that is a pointwise quantity, is an integral quantity and it allows to average out measurement errors like reflections. For example, by using the efficiency of the reference antenna, the calibration of the system becomes almost independent on the floor type (absorbing or conductive).

Since in absorber-based systems the power radiated in the lower hemisphere is absorbed, only the efficiency relevant to the upper hemisphere (upper hemisphere efficiency, UHE) should be considered during the calibration. The UHE is defined as follows:

$$UHE = \frac{1}{4\pi} \int_{\phi=0}^{2\pi} \int_{\theta=0}^{\pi/2} G(\theta, \varphi) \sin \theta d\theta d\varphi, \quad (1)$$

where  $G(\theta, \varphi)$  is the gain normalized pattern. As can be seen the  $\theta$ -integral is in this case computed in the angular range 0 and 90° (upper hemisphere) while for full efficiency the angular range is 0 and 180° (full sphere).

The full efficiency should instead be considered to calibrate the PEC-based systems. In fact, in such cases, the field on the lower hemisphere is fully reflected by the metallic floor and the total radiated power is thus collected.

Results from the calibration analysis performed in [15] are summarized in Fig. 4, where the calibration errors (i.e. delta between the calibration factor obtained in free-space condition and in absorber or conductive floor conditions) are shown for the gain (left) and efficiency (right) calibration methods. The green traces are calibration errors for the 18-inch absorbers. The red and black traces are calibration errors for the 48-inch absorbers (Abs48) and PEC floor (PEC), respectively.

As can be seen, the errors are much smaller when the efficiency calibration is applied (<0.2 dB at almost any frequency point and scenario; the larger calibration errors for the PEC-based measurements at 500 and 600 MHz are associated with other measurement errors of the implemented measurement setup, not to the calibration method itself). The efficiency is in fact an integral quantity and errors due to spurious radiations in the measurement setup tend to be averaged out. On the other hand, the gain is a pointwise quantity and hence is more subject to measurement errors.

### Gain pattern measurements

The performed spherical NF acquisitions of the three vehicle installed antennas in the different floor scenarios have been transformed to the far field (FF) with NF/FF transformations [3].

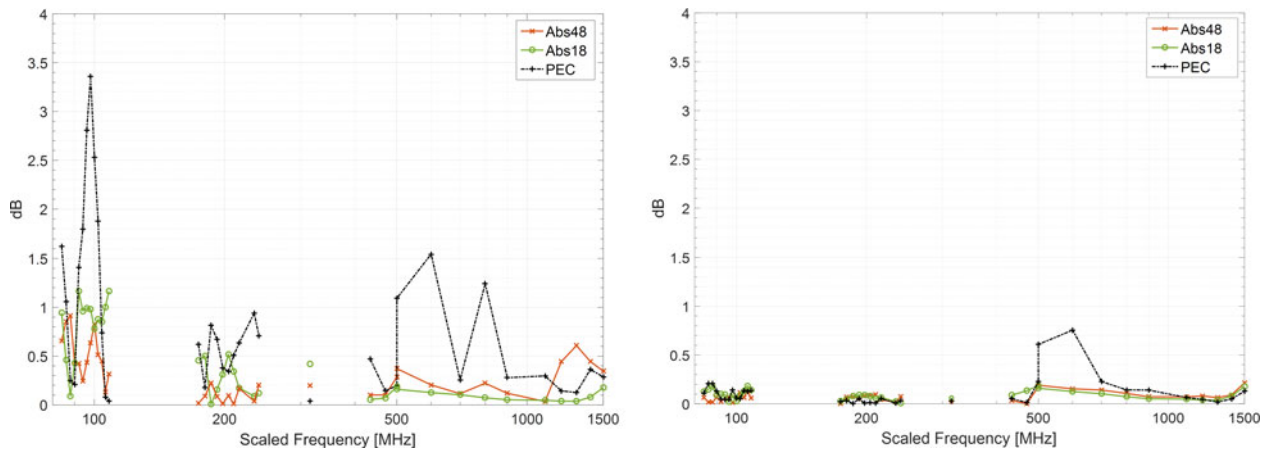


Fig. 4. Calibration error comparison: gain calibration (left); efficiency calibration (right).

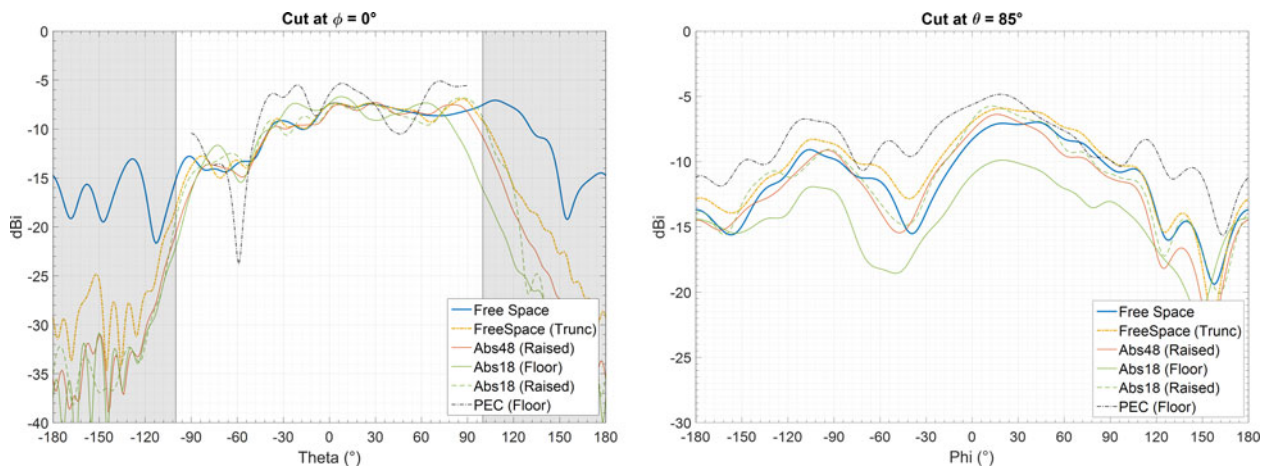


Fig. 5. Hood antenna: vertical (left) and horizontal (right) gain pattern comparison at 210 MHz (scaled frequency).

Free-space and absorber-based measurements have been processed with the conventional spherical wave expansion (SWE) NF/FF approach [3], simply considering zero-padding in the truncated areas. The PEC-based measurements have instead been processed enforcing the PEC boundary condition during the NF/FF [10]. To do that, the translated-SWE (TSWE) technique [16–18] has been used to translate the reference system along the z-axis to have the PEC interface at  $z = 0$  m. For each measurement configuration, the obtained patterns have been properly scaled with the gain calibration coefficients obtained during the calibrations of the system (one set of calibration coefficients for each floor scenario).

Gain pattern comparison at  $\phi = 0^\circ$  (i.e. cut along the vehicle’s longest dimension) and at 210 MHz (scaled from 2520 MHz) is reported in Fig. 5 (left) for the hood-antenna. The blue trace is the free-space measurement considered as the reference, while the black-dashed trace is the PEC-based one; the solid-red trace is the measurement performed over the 48-inch absorber; the solid-green and dashed-green traces are the measurements over the 18-inch absorbers in floor and raised configurations, respectively. Only the latter has also been post-processed with Mv-Echo tool [13], to mitigate the effect of the degraded reflectivity of the absorbers (spatial filtering). The shadowed areas indicate the

unreliable FF regions associated to the scan truncation (at  $100^\circ$ ). As expected, the deviations between the free-space and the PEC-based measurements are quite large. Instead, measurements over the 48-inch absorbers agree well with the free-space especially within  $|\theta| \leq 90^\circ$  (no spatial filtering is applied to this measurement). More deviations are instead observable when the car is measured over the 18-inch absorber in the floor configuration. This is due to the unsatisfactory reflectivity of the absorbers which is greater than  $-20$  dB at this frequency (see Table 1). It should be noted that in such case, due to the reduced equivalent  $\theta$ -scanning area (see Fig. 3), the pattern levels drop down at smaller  $\theta$  angles than in the case of the measurements with the 48-inch absorbers. Instead, by raising the car over the 18-inch absorbers, the pattern exhibits a level comparable to free-space up to larger  $\theta$  angles. Moreover, for the raised vehicle, the increased electrical distance with respect to the floor and the application of the spatial filtering with Mv-Echo improve the agreement with the free-space.

The yellow trace is obtained from the free-space near-field measurement truncated at  $\theta = 100^\circ$  and it has been added to the comparison to isolate the truncation effect from the effect of the different floors. As described in [11], the truncation errors are an artifact introduced during the NF/FF transformation and

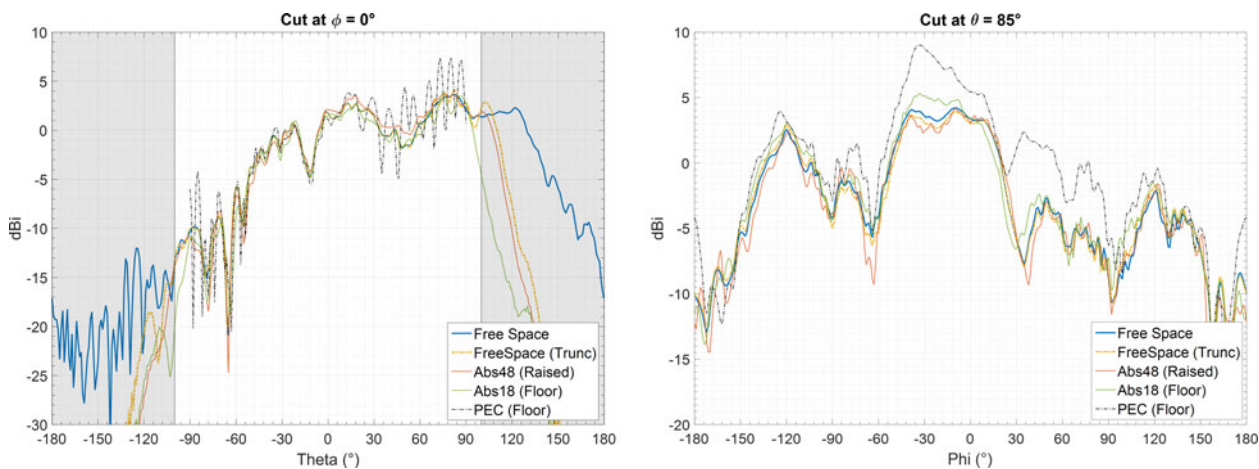


Fig. 6. Hood antenna: vertical (left) and horizontal (right) gain pattern comparison at 1200 MHz (scaled frequency).

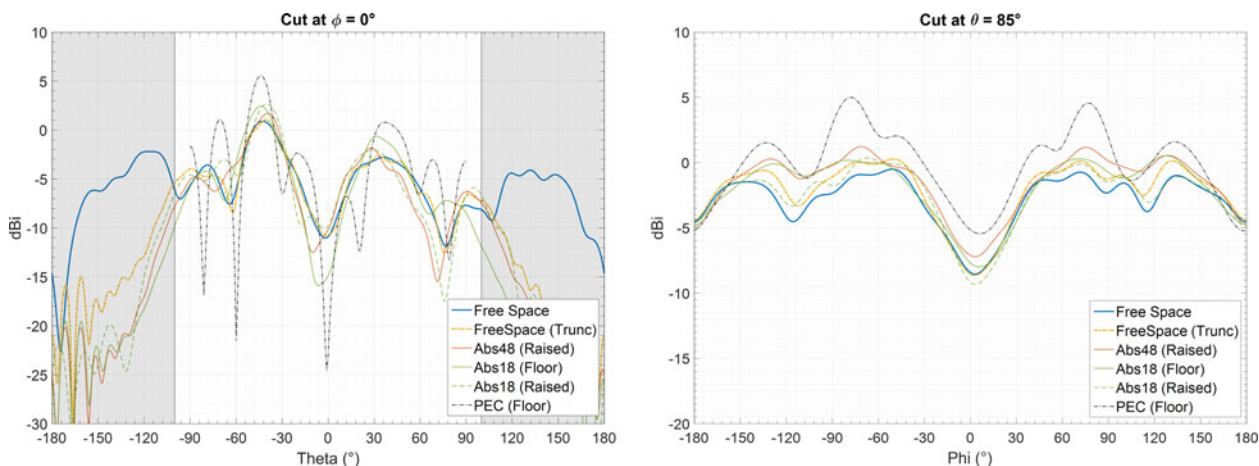


Fig. 7. Rear roof antenna: vertical (left) and horizontal (right) gain pattern comparison at 210 MHz (scaled frequency).

could propagate to different regions of the transformed pattern, especially at lower frequencies. As expected, the truncation of the scanning area at such low frequency generates a ringing effect which increases when approaching the truncation angle ( $\theta = 100^\circ$ ).

Considering again the hood antenna, a similar comparison is reported in Fig. 5 (right) for the horizontal cut at  $\theta = 85^\circ$ . Even along this cut, the two raised measurements agree well with the free-space, while more deviations are observed in case of floor measurements over PEC and 18-inch absorbers.

Vertical ( $\phi = 0^\circ$ ) and horizontal ( $\theta = 85^\circ$ ) pattern comparisons of the hood antenna along the same two cuts previously shown at 210 MHz are reported in Fig. 6 at 1200 MHz. In this case, the interaction with the conductive floor is more evident with respect to the measurement performed at 210 MHz, resulting in a vertical pattern with a significant ripple. It should be noted that the interaction with a PEC floor can also be largely mitigated by applying a spatial filtering [9, 13]. Such mitigation is more effective at higher frequencies (e.g. 1200 MHz) if the car is raised from the PEC floor. More details and examples regarding this topic can be found in [9]. On the other hand, at this frequency, both absorbers exhibit a low reflectivity (see Table 1); therefore, the agreement of absorber-based systems with the free-space

measurements is good. Moreover, also at this frequency, a larger reliable FF area is obtained with the measurement over the 48-inch absorber. In fact, in such a case, the vehicle was raised from the floor, achieving a larger equivalent  $\theta$  scanning (see also Fig. 3). Instead, with the 18-inch absorber, the vehicle was on the floor, resulting in a reduced equivalent  $\theta$  scanning. Finally, as expected [11], the truncation errors are now less pronounced at this higher frequency (see yellow traces).

Similar gain pattern comparisons presented for the hood antenna are shown in Figs 7 and 8 for the rear roof antenna. Even though the measured radiation patterns are different because of the different antenna positions within the body of the scaled vehicle, the comments previously reported apply also in this case.

The different measurement configurations and measured antennas are compared over the whole frequency band, considering the equivalent noise level (ENL) defined as

$$ENL = 20 \log_{10} \left( RMSE \left| \frac{E(\theta, \phi) - \tilde{E}(\theta, \phi)}{E(\theta, \phi)_{MAX}} \right| \right), \quad (2)$$

where  $E(\theta, \phi)$  is the reference gain pattern (free-space),  $\tilde{E}(\theta, \phi)$  is the test gain pattern, and RMSE stands for root mean square error.



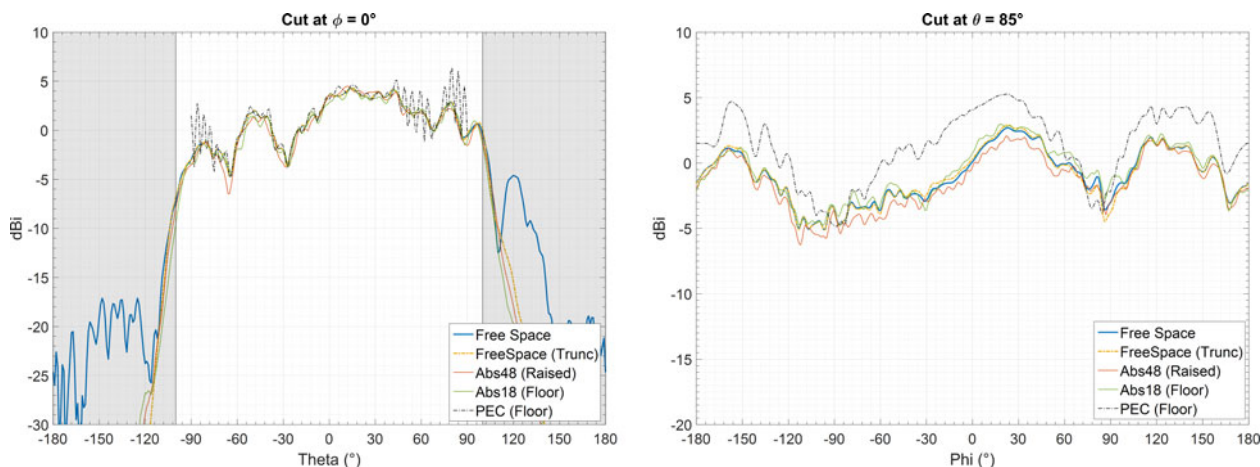


Fig. 8. Rear roof antenna: vertical (left) and horizontal (right) gain pattern comparison at 1200 MHz (scaled frequency).

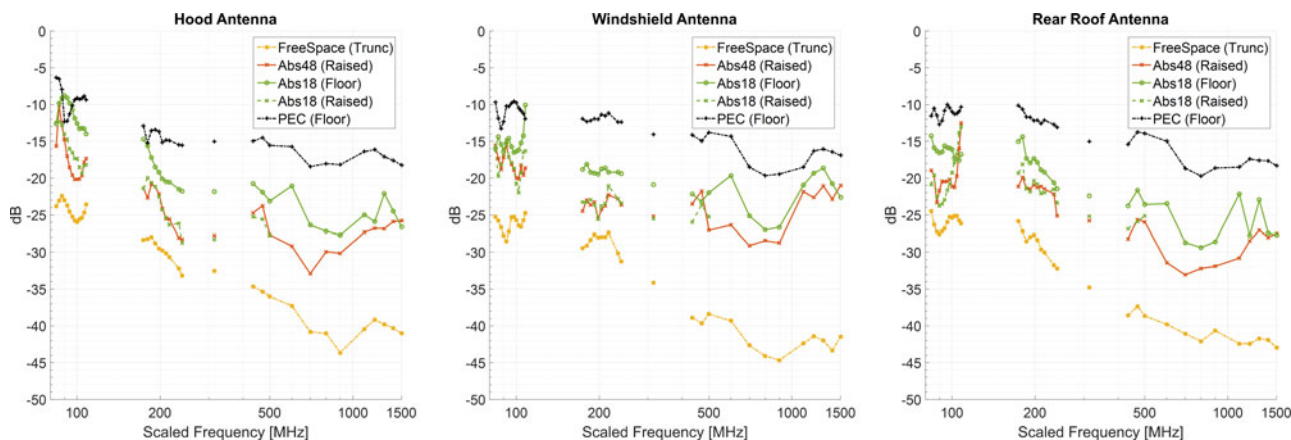


Fig. 9. Equivalent noise level (ENL) comparison among the different scenarios and antennas: hood antenna (left); windshield antenna (center); rear-roof antenna (right).

The ENL has been evaluated over the whole upper hemisphere (from the zenith down to the horizon) and over the full  $\phi$  range (from 0 to 360°). The ENL comparisons are reported in Fig. 9 for the hood (left), windshield (center), and rear-roof antenna (right). The same color convention previously used for the pattern comparison has also been adopted here. The large deviations of the PEC-based measurements from free-space are confirmed over the entire frequency range and for each antenna position. As expected, a much better agreement with the free-space is reached when the 48-inch absorbers are used (it is remarked that no spatial filtering is applied to this measurement). The performances of the 18-inch absorbers with the car placed on the floor are poorer at lower frequencies, and gradually improve with the increasing frequency. In this case, the performances at lower frequencies cannot be improved by spatial filtering because the car is too close to the floor. Instead, if the car is raised over the 18-inch absorbers and the spatial filtering is applied, performances improve also at lower frequencies, almost reaching the same error level obtained with the bigger absorbers. This interesting behavior is observed for each considered antenna position. It is finally observed that the ENLs obtained when truncated free-space measurements are investigated are much lower because only one error contribution (the truncation error) is present. As

Table 2. Peak gain deviations from full-spherical free-space scenario (P2P RMS errors in dB)

Scenario	84–315 MHz	434–1500 MHz
Free-space (trunc.)	0.8	0.2
Abs48 (raised)	1.8	0.8
Abs18 (floor)	2.8	1.2
Abs18 (raised)	1.9	–
PEC (floor)	4.2	2.4

expected, the effect of truncation errors is higher at lower frequencies and gradually decreases at higher frequencies [11].

The deviation of the peak gain for the different floors and the truncated free-space scenarios with respect to the full-spherical free-space configuration is shown in Table 2. This estimation has been divided into two frequencies sub-bands: low band (LF, 84–315 MHz) and high band (HF, 434–1500 MHz). From the ENLs previously computed, for each frequency point and antenna position, the corresponding peak-to-peak (P2P) errors at the maximum of the (gain) patterns have been estimated. The root mean square (RMS) has been computed considering

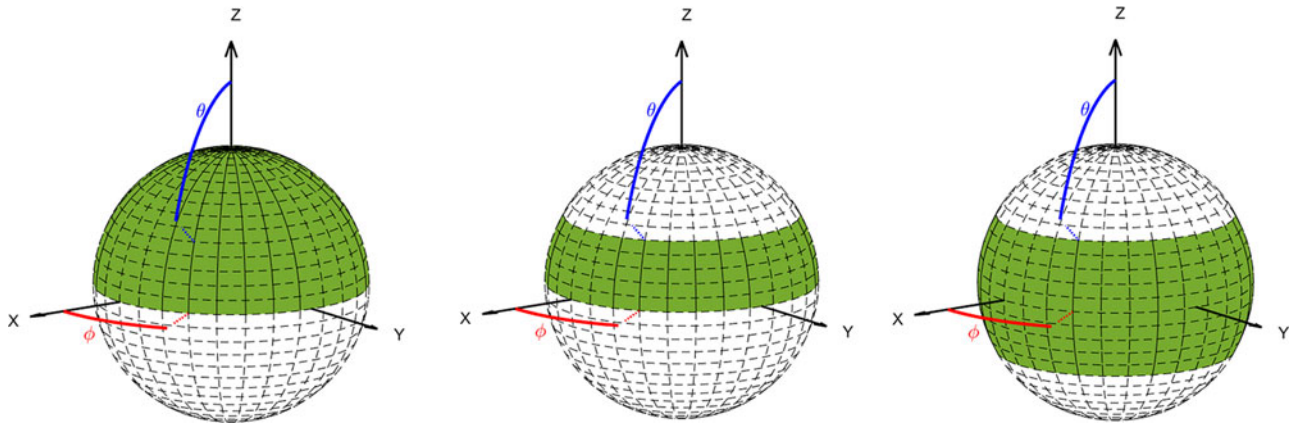


Fig. 10. Illustration of the integration domain for the UHRP (left), N75PRP (center), and NHPRP (right).

in each sub-band all frequencies and all antenna positions. It should be noted that in the LF band, the performances of the 48-inch absorbers measurements and the one with the 18-inch absorbers with the raised vehicle are comparable. Deviations are instead higher if the 18-inch absorbers are used with the vehicle on the floor. As expected, the highest deviations are obtained with the PEC floor on both sub-bands. It is finally observed that the truncation errors have a smaller impact with respect to the floor effect and as expected, such impact is smaller in the higher frequency band.

### Partial radiated powers

For automotive communications, it is not the total radiated power (TRP) that is critical. There are specific angular ranges over which each technology operates, and this is reflected by the figure of merits defined in the 5G Automotive Association (5GAA) [19]. In fact, in the 5GAA standard different Partial Radiated Powers (PRP) are defined.

In this study, the effect of the used floor scenarios on the evaluation of three different PRP defined in the standard are analyzed, namely: the Upper Hemisphere Radiated Power (UHRP), the Near 75 degrees Partial Radiated Power (N75PRP) and the Near Horizon Partial Radiated Power (NHPRP).

PRPs are computed in far field integrating the Effective Isotropic Radiated Power (EIRP) on the complete  $\phi$  range ( $\phi = [0, 2\pi)$ ) and a portion of the  $\theta$  range ( $\theta = [\theta_{min}, \theta_{max}]$ ) as shown in the following equation and illustrated in Fig. 10.

$$PRP = \frac{1}{4\pi} \int_{\phi=0}^{2\pi} \int_{\theta=\theta_{min}}^{\theta_{max}} EIRP(\theta, \phi) \sin \theta d\theta d\phi \quad (3)$$

In particular:

- For the UHRP, the  $\theta$ -integral ranges from  $\theta_{min} = 0^\circ$  to  $\theta_{max} = 90^\circ$
- For the N75PRP, the  $\theta$ -integral ranges from  $\theta_{min} = 60^\circ$  to  $\theta_{max} = 90^\circ$
- For the NHPRP, the  $\theta$ -integral ranges from  $\theta_{min} = 60^\circ$  to  $\theta_{max} = 120^\circ$

When the antennas are tested together with their generator (Over-The-Air measurements, [19–21]) and the measurement

system is properly calibrated, the above partial radiated powers are indeed measured and are expressed in dBm. Instead, in this analysis, passive measurements are performed using a Vector Network Analyzer (VNA), hence the obtained partial radiated powers are normalized to the input power. In other words, the corresponding partial efficiencies, computed as the partial integrals of the gain patterns (instead of the EIRP), have been considered. The different floor scenarios will affect the partial efficiencies and the partial radiated powers in the same way, hence, in the following, without loss of generality, we refer to the latter, even though the former have been computed.

The differences of the UHRP, N75PRP and NHPRP evaluated on the different floors with respect to the corresponding free-space metrics have been computed:

$$\begin{aligned} \Delta UHRP &= UHRP_{floor} - UHRP_{free-space} \\ \Delta N75PRP &= N75PRP_{floor} - N75PRP_{free-space} \\ \Delta NHPRP &= NHPRP_{floor} - NHPRP_{free-space} \end{aligned}$$

Such deltas are plotted in Fig. 11 for the hood antenna. The same color convention previously used for the ENL has also been adopted here. As can be seen, the PEC floor overestimates UHRP and N75PRP, as in fact, the power radiated toward the floor is re-radiated in the upper hemisphere. Good UHRP agreements with the free-space are instead obtained for each measurement performed over the absorbing floors. The UHRP is an integral quantity and hence is robust against measurement perturbation such as ground reflections and truncation errors [11] as discussed in [15]. The N75PRP is instead obtained integrating a smaller domain hence it becomes more sensitive to measurement perturbations. The N75PRP results obtained with the 18-inch absorbers with the car on the floor are in fact worse than the corresponding UHRP results. The N75PRP results obtained with the 48-inch absorbers and with the 18-inch absorber with the raised vehicle are instead comparable with the corresponding UHRP results.

The NHPRP has been defined in the 5GAA standard to ease the comparison between the PEC-based and absorbed-based systems. When the NHPRP is computed from PEC-based systems is equivalent to integrate from  $\theta_{min} = 60^\circ$  to  $\theta_{max} = 90^\circ$  (because there is no field beyond  $90^\circ$ ) but, due to the presence of the PEC, the power that would be radiated in the  $\theta = [90^\circ - 120^\circ]$  range is radiated back in the  $\theta = [60^\circ - 90^\circ]$  range. Hence, the



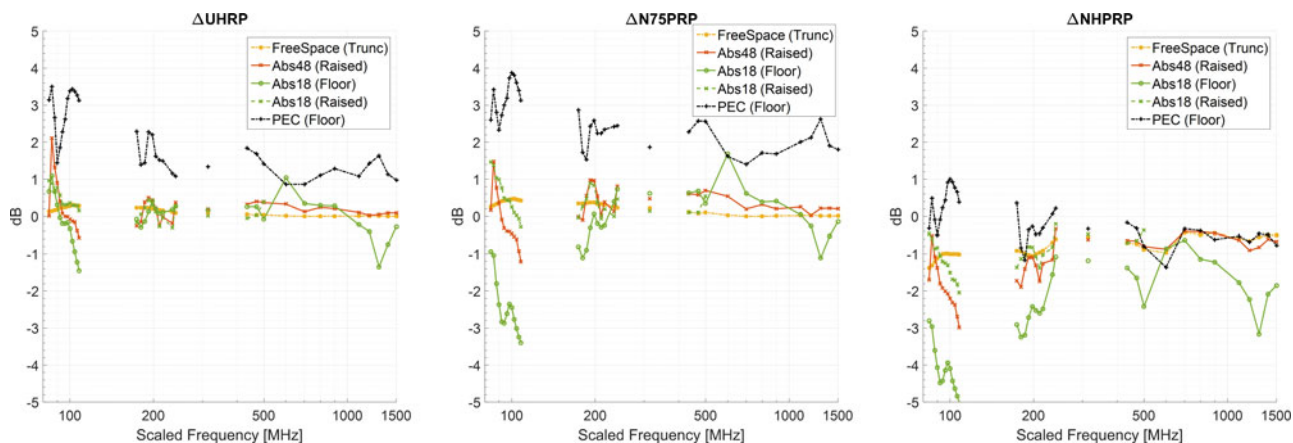


Fig. 11. Hood antenna PRPs: deviation of the different scenarios from the free-space; ΔUHRP (left), ΔN75PRP (center), ΔNHPRP (right).

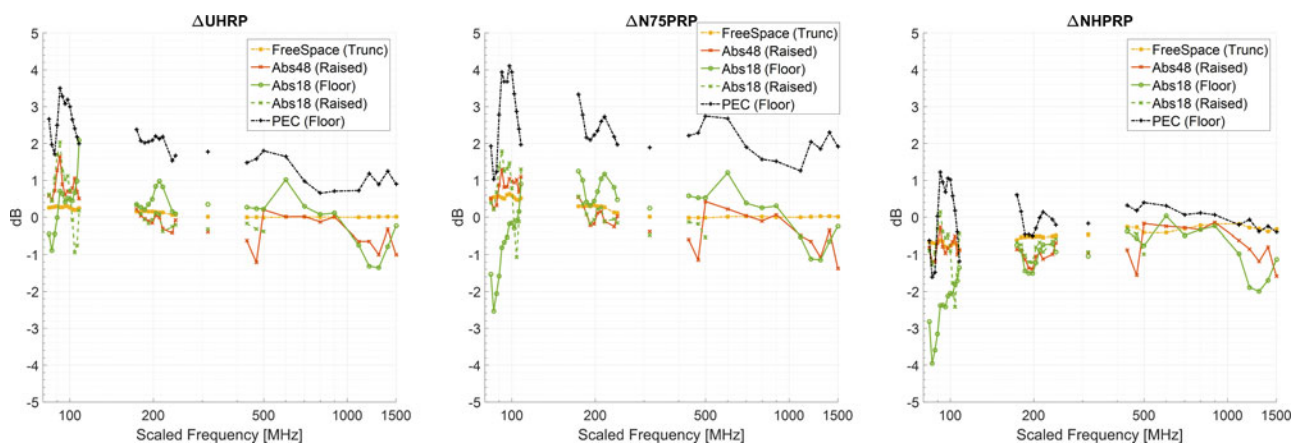


Fig. 12. Windshield antenna PRPs: deviation of the different scenarios from the free-space; ΔUHRP (left), ΔN75PRP (center), ΔNHPRP (right).

NHPRP parameter should lend itself to a better comparison between the PEC-based and free-space case. As expected, the NHPRP calculated from measurements with the PEC floor scenario are closer to those computed in free-space conditions (see black trace of Fig. 11, right). Larger, and negative deviations are instead obtained when the NHPRP are evaluated with the different absorber floors and even with the truncated free-space scenario (see yellow trace). This is due to the fact that in the experiment the spherical acquisitions have been truncated at  $\theta = 100^\circ$ , while the NHPRP is obtained integrating up to  $120^\circ$ . Consequently, the values of NHPRP are underestimated.

Similar UHRP, N75PRP and NHPRP results are shown in Figs 12 and 13 for the windshield and rear-roof antenna, respectively.

The differences of the partial radiated powers with respect to the free-space scenario have been used to statistically analyze and summarize the results. As done previously for the peak gain investigation, this analysis has been divided into two frequencies sub-bands: LF (84–315 MHz) and HF (434–1500 MHz). For each floor configuration and each metric, the mean value ( $\mu$ ) and the standard deviation ( $\sigma$ ) of the differences have been computed considering different frequencies and all three different antenna positions. Results are reported in Tables 3 and 4 for the LF and HF band, respectively.

- *Truncated free-space scenario*: these measurements slightly overestimate the UHRP and N75PRP at LF while at HF the mean values and standard deviation are less than 0.1 dB. These observed non-zero deviations are due to the propagation of the truncation errors introduced during the NF/FF transformation. The NHPRP instead is underestimated both at LF and HF because of the power lost in the truncated region.
- *48-inch absorbers*: ΔUHRP and ΔN75PRP have a mean value very close to 0 dB and a maximum standard variation of 0.6 dB at LF and 0.5 at HF. The NHPRP is underestimated especially at LF.
- *18-inch absorbers with the vehicle on the floor*: the ΔUHRP are comparable to the ones computed with the 48-inch absorbers both at LF and HF. In fact, the relatively large integration domain allows to average out the perturbations caused by the limited absorbing properties of the 18-inch absorbers. Larger N75PRP deviations are instead observed because for such a metric the integration domain is smaller. The NHPRP deviations are larger than those obtained considering the 48-inch scenario because in that case the vehicle is raised hence, the amount of radiated power lost in the truncated area is reduced.
- *18-inch absorbers with raised vehicle*: UHRP, N75PRP and NHPRP results are all comparable to the ones obtained with the 48-inch absorbers.

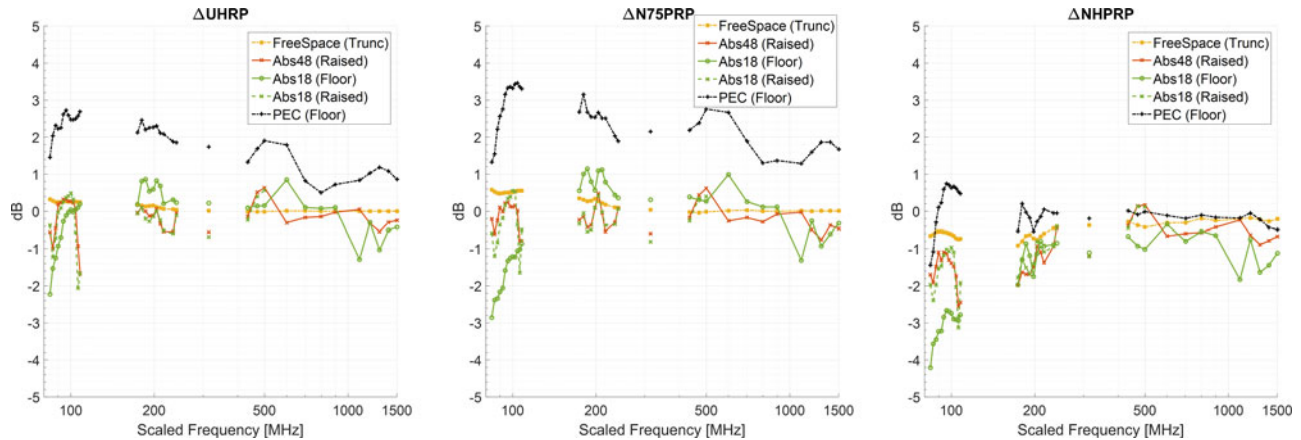


Fig. 13. Rear roof antenna PRPs: deviation of the different scenarios from the free-space;  $\Delta$ UHRP (left),  $\Delta$ N75PRP (center),  $\Delta$ NHPRP (right).

Table 3. Statistical analysis of the deltas of the PRPs evaluated in the different scenarios with respect to the free-space: 84–315 MHz frequency band

Scenario	$\Delta$ UHRP		$\Delta$ N75PRP		$\Delta$ NHPRP	
	$\mu$ (dB)	$\sigma$ (dB)	$\mu$ (dB)	$\sigma$ (dB)	$\mu$ (dB)	$\sigma$ (dB)
Free-space (trunc.)	+0.2	0.1	+0.4	0.1	-0.7	0.3
Abs48 (raised)	+0.1	0.6	+0.1	0.6	-1.3	0.6
Abs18 (floor)	+0.1	0.7	-0.7	1.3	-2.4	1.2
Abs18 (raised)	+0.1	0.7	+0.2	0.7	-1.1	0.6
PEC (floor)	+2.3	0.6	+2.7	0.7	+0.0	0.6

Table 4. Statistical analysis of the deltas of the PRPs evaluated in the different scenarios with respect to the free-space: 434–1500 MHz frequency band

Scenario	$\Delta$ UHRP		$\Delta$ N75PRP		$\Delta$ NHPRP	
	$\mu$ (dB)	$\sigma$ (dB)	$\mu$ (dB)	$\sigma$ (dB)	$\mu$ (dB)	$\sigma$ (dB)
Free-space (trunc.)	+0.0	0.0	+0.0	0.0	-0.4	0.2
Abs48 (raised)	-0.1	0.4	-0.1	0.5	-0.6	0.4
Abs18 (floor)	-0.1	0.6	+0.1	0.7	-1.2	0.7
Abs18 (raised)	-	-	-	-	-	-
PEC (floor)	+1.2	0.4	+2.0	0.4	-0.2	0.4

- *PEC floor*: the UHRP and the N75PRP are overestimated both at LF and HF. Again, this is due to the fact that the power radiated toward the floor is re-radiated in the upper hemisphere. The  $\Delta$ NHPRP has a mean value very close to 0 dB both at LF and HF and the standard deviation is 0.6 dB at maximum. The NHPRP computed on PEC scenarios is identical to the N75PRP because no power is radiated on the backward hemisphere, and as expected, compares well with the NHPRP computed on the (untruncated) free-space scenario.

## Conclusion

Scaled automotive measurements have been conducted to compare the measurement performances of absorber- and PEC-based spherical near-field systems in the 84–1500 MHz

frequency range. Measurements in free-space conditions have been considered as the reference.

Three configurations have been investigated: two scaled absorbers emulating 48-inch and 18-inch height full-scale absorbers, and a conductive floor. The 48-inch absorbers provide better performances at lower frequencies, but they are more expensive and lead to longer measurement setup phases because they are more difficult to handle and imply measurements with the car raised from the ground. On the other hand, the 18-inch absorbers would allow for faster measurement setups, but with a higher measurement uncertainty at lower frequencies, due to their poorer reflectivity. As a practical compromise, scaled measurements with the 18-inch absorbers at lower frequencies have also been performed with the car raised from the floor, to reduce the interaction with the floor itself and to apply a spatial filtering in

post-processing. The main advantage of the PEC-based measurements is the ease of the accommodation of the vehicle, which is normally simply placed in the center of the system.

Considering the free-space scenario as the reference, it has been shown that conductive floor systems lead to the largest gain deviations because of the stronger interaction with the conductive floor. Similarly, the UHRP and N75PRP are overestimated. Instead, the NHPRP evaluated over the conductive floor is the closest to the one measured in free-space.

As expected, the scaled measurement with the 48-inch absorbers exhibits the best agreement with the free-space for the gain, the UHRP and the N75PRP. The NHPRP is instead underestimated because of the truncation of the scanning spherical surface.

At higher frequencies, the performances obtained with measurements conducted with the 18-inch absorbers are comparable with the one obtained with the 48-inch absorbers for all the evaluated figure of merits. As expected, the performances of the 18-inch absorber degraded at lower frequencies. Finally, it has been shown that by raising the vehicle from the floor and applying a spatial filtering, it is possible to improve the quality of the measurements with 18-inch absorbers at lower frequencies for all investigated metrics and reach approximately the same uncertainty of the measurement of the 48-inch absorbers.

## References

- Saccardi F, Mioc F, Giacomini A, Scannavini A, Foged LJ, Estrada J, Iversen PO, Edgerton M and Graham JA (2020) Experimental comparison of vehicular antenna measurements performed over different floors. *2020 14th European Conference on Antennas and Propagation (EuCAP)* (<https://ieeexplore.ieee.org/document/9135819>, 10.23919/EuCAP48036.2020.9135819).
- Recommended Practice for Near-Field Antenna Measurements, IEEE Std 1720-2012.
- Hansen JE (ed.) (1988) *Spherical Near-Field Antenna Measurements*, Peter Peregrinus Ltd., on behalf of IEE, London, United Kingdom.
- Noren P, Garreau P and Foged LJ (2012) State of the art spherical near-field antenna test systems for full vehicle testing. *EuCAP*, Prague, Czech Republic, March 2012.
- Asghar ME, Wollenschläger F, Bornkessel C, Griesche A and Hein MA (2019) Comparative analysis of spherical near-field automotive antenna measurement facilities. *2019 13th European Conference on Antennas and Propagation (EuCAP)*.
- Saccardi F, Mioc F, Giacomini A and Foged LJ (2018) Estimation of the Realistic ground effect in free-space automotive measurements. *40th AMTA Symposium, Williamsburg, Virginia, USA*, Nov 2018.
- Saccardi F, Mioc F, Foged LJ, Iversen PO and Estrada J (2020) Estimation of real ground effect in absorber-based automotive measurements: experimental validation. *APS 2020, 5–10 July 2020, Montréal, Canada*.
- Scialacqua L, Foged LJ, Mioc F and Saccardi F (2017) Link between measurement and simulation applied to antenna scattering and placement problems. *EuCAP, Paris, France, 19–24 March 2017*.
- Saccardi F, Mioc F, Estrada J, Iversen PO, Foged LJ, Edgerton M and Graham JA (2019) Comparative investigation of spatial filtering techniques for ground plane removal in PEC-based automotive measurements. *AMTA, San Diego, CA, USA, 6–11 October 2019*.
- Mauermayer RAM and Eibert TF (2016) Spherical field transformation for hemispherical antenna measurements above perfectly conducting ground planes. *AMTA, Austin, TX, USA, October 2016*.
- Saccardi F, Rossi F, Scialacqua L and Foged LJ (2017) Truncation error mitigation in free-space automotive partial spherical near field measurements. *AMTA, Atlanta, GA, USA, 15–20 October 2017*.
- <https://www.mvg-world.com/en/products/antenna-measurement/software/mv-echo> (accessed July 2021).
- Standard Test Procedures for Antennas, ANSI/IEEE Std 149-1979.
- Saccardi F, Mioc F, Giacomini A, Scannavini A, Foged LJ, Estrada J, Iversen PO, Edgerton M and Graham JA (2019) Accurate calibration of truncated spherical near field systems with different ground floors using the substitution technique. *AMTA, San Diego, CA, USA, 6–11 October 2019*.
- Foged LJ, Saccardi F, Mioc F and Iversen PO (2016) Spherical near field offset measurements using downsampled acquisition and advanced NF/FF transformation algorithm. *EuCAP, Davos, Switzerland, 10–15 April 2016*.
- Saccardi F, Mioc F, Iversen PO, Estrada J and Foged LJ (2020) Experimental validation of the translated-SWE technique applied to automotive measurements over PEC-floor at arbitrary height. *2020 14th European Conference on Antennas and Propagation (EuCAP)*.
- Wollenschläger F, Foged LJ, Asghar ME, Bornkessel C and Hein MA (2019) Spherical wave expansion applied to the measured radiation patterns of automotive antennas in the installed state in the GHz range. *2019 13th European Conference on Antennas and Propagation (EuCAP)*, pp. 1–5.
- G Automotive Association (5GAA); DRAFT TR P-210024 Working Group Evaluation, test beds and pilots Vehicular Antenna Test Methodology.
- Asghar ME, Bornkessel C and Hein MA (2020) Experimental determination of the total radiated power of automotive antennas in the installed state. *2020 14th European Conference on Antennas and Propagation (EuCAP)*, pp. 1–5.
- Pelland P, van Rensburg DJ, Berbeci M, Storjohann FO, Griesche A and Busch J-P (2020) Automotive OTA measurement techniques and challenges. *2020 Antenna Measurement Techniques Association Symposium (AMTA)*, pp. 1–6.



Francesco Saccardi received the M.Sc. degree in telecommunication engineering from the University of Siena in 2010. He performed his thesis activity on antenna measurements at the Denmark Technical University (DTU). In October 2010, he joined the Microwave Vision Group (MVG) where he is currently working in the R&D department. His activities are mainly focused on the research and development of innovative antenna measurement techniques for several applications. He has authored and coauthored more than 70 journal and conference papers on antenna measurement and related post-processing techniques. He also contributed to the writing of the book “Post-processing techniques in Antenna Measurements”. In 2013, he and his colleagues received the AMTA “Best Technical Paper Award”. He has taught in several seminars and workshops focused on general near-field antenna measurements, automotive measurements, and advanced post-processing techniques. Since 2020, he is a senior member of AMTA.



Francesca Mioc received the M.Sc. and Ph.D. degrees in electronic engineering from the University of Florence (Italy). From 2000 to 2002, she was working with Ingegneria Dei Sistemi S.p.A. (IDS) as a Senior Engineer at Aerospace Division. From 2002 to 2008, she was working as a Senior Technical Staff at SATIMO Italy where she was technical responsible for software R&D for measurement post-processing (near to far field transformation, antenna parameters, back-propagation, holography), antenna diagnostic from measurements and electromagnetic propagation in complex environments. She was also leader of the European working group for the definition of a data format for the exchange of electromagnetic field data, project co-founded by ESA and European Commission within the Sixth Framework Program (2005-2006). Since 2009 she has been working as a consultant for general antenna developments involving, measurement post processing, antenna diagnostic and data standardization.





**Alessandro Scannavini** received his M.S. degree in electronic engineering from University La Sapienza, Roma, Italy in 2000. He was with Motorola Design Center, in Turin (Italy), and Chicago (USA) from 2000 to 2006. He was involved in designing antenna and RF components for 2G and 3G products. He joined MVG (formerly SATIMO) in 2007 as Field Application Engineer. In MVG, he worked with

R&D team on new technologies to be used for designing accurate and fast antenna measurement systems and was involved in pre-sale and after sale activities. Since 2009, he is a 3GPP (3G Partnership Project) and CTIA-The Wireless Industry delegate. He actively contributed to the MIMO OTA test plan, and 3GPP AAS BS OTA specifications with authoring and co-authoring more than 50 contributions. He is now working on 5G solutions for OTA measurements at sub6 GHz and mmWave and actively contributing to the standard for NR UE performance testing. He is currently the Standardization Specialist of the MVG.



**Per Olav Iversen** is the CTO of MVG. Per earned his MSEE degree from the University of California, Los Angeles and his BSEE degree from California State University, Long Beach. He started his career at LJR (now Optim Microwave). In 1991, he moved to the Netherlands to work at ESA/ESTEC. In 1998, he joined SATIMO as Technical Director, where he helped develop and commercialize

their probe array technology. In 2008, as part of a corporate merger, he became the CEO of MVG-Orbit/FR, Inc. He has been a contributing member to various international standardization committees (CTIA, WiMax Forum, Wi-Fi Alliance). He is a senior member of AMTA and has served on its Board of Directors as Secretary and Vice President. He is a regular lecturer for the UCLA Extension course on "Modern Microwave Antenna Measurements". He has co-authored numerous papers mainly related to multiprobe antenna measurement and is currently involved in developing test systems for 5G and millimeter-wave antenna applications.



**John Estrada** earned his Bachelor of Electrical Engineering from Auburn University, and his MSEE from the Georgia Institute of Technology. He has been active in the field of antenna measurements for more than 35 years, working at the Georgia Tech Research Institute and MVG/Satimo for the entirety of his career. Estrada is currently the CEO for the MVG office in Atlanta, GA, and is also the MVG Sales

Director for the Americas. He is a Senior Member of the Antenna Measurement Techniques Association (AMTA), formerly served on the AMTA Board of Directors from 2014 to 2016 in the roles of Meeting Coordinator and Vice President, and currently serves on the IEEE AP-S Technical Committee on Antenna Measurements (TCAM). He remains actively involved in the antenna engineering community, participating in various standardization groups and international committees, and has authored and co-authored numerous papers on antenna measurements and modeling techniques.



**Lars Jacob Foged** is Scientific Director of the Microwave Vision Group. Since 2004, he was secretary and now vice-chair of the IEEE Antenna Standards Committee. He is a board member and teacher in the European School of Antennas (ESOA) since 2006. He was a member of the EURAAP Delegate Assembly from 2009 to 2012 and Vice-Chair of the EuCAP conference in 2011 and 2022.

In 2016 and 2017, he led the Industry Initiatives Committee (IIC) of IEEE APS. He is a Board Member, Fellow and Distinguished Achievement Award recipient of AMTA. He has authored or co-authored more than 300 journal and conference papers on antenna design and measurement topics and received the "Best Technical Paper Award" at the 2012 AMTA Symposium and the "Best Measurement Paper Award" at the EuCAP 2021 conference. He contributed to six books and standards and hold four patents.